

TOPICAL REVIEW • OPEN ACCESS

Emerging inorganic solar cell efficiency tables (Version 1)

To cite this article: Lydia H Wong *et al* 2019 *J. Phys. Energy* 1 032001

View the [article online](#) for updates and enhancements.



TOPICAL REVIEW

Emerging inorganic solar cell efficiency tables (Version 1)

OPEN ACCESS

RECEIVED

29 March 2019

REVISED

17 May 2019

ACCEPTED FOR PUBLICATION

21 May 2019

PUBLISHED

29 July 2019

Original content from this work may be used under the terms of the [Creative Commons Attribution 3.0 licence](#).

Any further distribution of this work must maintain attribution to the author(s) and the title of the work, journal citation and DOI.



Lydia H Wong¹ , Andriy Zakutayev² , Jonathan D Major³ , Xiaojing Hao⁴ , Aron Walsh^{5,6} , Teodor K Todorov⁷ and Edgardo Saucedo^{8,9}

¹ Nanyang Technological University, 637553 Singapore, Singapore

² National Renewable Energy Laboratory, Golden, Colorado 80401, United States of America

³ University of Liverpool, Liverpool, L69 7ZF, United Kingdom

⁴ University of New South Wales, Sydney, NSW 2052, Australia

⁵ Imperial College London, London SW7 2AZ, United Kingdom

⁶ Yonsei University, Seoul 03722, Republic of Korea

⁷ IBM Thomas J. Watson Research Center, New York 10598, United States of America

⁸ Catalonia Institute for Energy Research (IREC), E-08930 Sant Adrià del Besòs- Barcelona, Spain

⁹ Author to whom any correspondence should be addressed.

E-mail: lydiawong@ntu.edu.sg, andriy.zakutayev@nrel.gov, jon.major@liverpool.ac.uk, xj.hao@unsw.edu.au, a.walsh@imperial.ac.uk, tktdoro@us.ibm.com and esaucedo@irec.cat

Keywords: thin film inorganic photovoltaics, emerging photovoltaic technologies, solar energy, photovoltaic conversion efficiency tables

Abstract

This paper presents the efficiency tables of materials considered as emerging inorganic absorbers for photovoltaic solar cell technologies. The materials collected in these tables are selected based on their progress in recent years, and their demonstrated potential as future photovoltaic absorbers. The first part of the paper consists of the criteria for the inclusion of the different technologies in this paper, the verification means used by the authors, and recommendation for measurement best practices. The second part details the highest world-class certified solar cell efficiencies, and the highest non-certified cases (some independently confirmed). The third part highlights the new entries including the record efficiencies, as well as new materials included in this version of the tables. The final part is dedicated to review a specific aspect of materials research that the authors consider of high relevance for the scientific community. In this version of the Efficiency tables, we are including an overview of the latest progress in theoretical methods for modeling of new photovoltaic absorber materials expected to be synthesized and confirmed in the near future. We hope that this emerging inorganic Solar Cell Efficiency Tables (Version 1) paper, as well as its future versions, will advance the field of emerging photovoltaic solar cells by summarizing the progress to date and outlining the future promising research directions.

Abbreviations

Eff. (%)	Conversion efficiency obtained under AM1.5 illumination in percentage
V_{OC} (V)	Open circuit voltage in Volts
J_{SC} (mA cm ⁻²)	Short circuit current in mili-Ampers by square centimeter
F. F. (%)	Fill factor in percentage
E_g (eV)	Bandgap in electronvolt
AZO	ZnO:Al
ITO	In ₂ O ₃ :SnO ₂
Spiro-OMeTAD	2,2',7,7'-Tetrakis[N,N-di(4-methoxyphenyl)amino]-9,9'-spirobifluorene (C ₈₁ H ₆₈ N ₄ O ₈)
TBAI	Tetrabutylammonium iodide

EDT	1,2-ethanedithiol
PTB7	Poly[[4,8-bis[(2-ethylhexyl)oxy]benzo[1,2-b:4,5-b']dithiophene-2,6-diyl][3-fluoro-2-[(2-ethylhexyl)carbonyl]thieno[3,4-b]thiophenediyl]] ((C ₄₁ H ₅₃ FO ₄ S ₄) _n)
ARC	Anti-reflection coating
CuPc ⁺	Copper phthalocyanine
PTAA	Poly[bis(4-phenyl)(2,4,6-trimethylphenyl)amine ((C ₂₁ H ₁₉ N) _n)
PCBM	[6,6]-Phenyl C61 butyric acid methyl ester (C ₇₂ H ₁₄ O ₂)
mp-TiO ₂	Mesoporous TiO ₂
PCPDTBT	poly[N-9'-heptadecanyl-2,7-carbazole-alt-5,5-(4,7-di-2-thienyl-2',1',3'-benzothiadiazole] ((C ₄₃ H ₄₇ N ₃ S ₃) _n C ₁₂ H ₁₀)
PEDOT:PSS	Poly(2,3-dihydrothieno-1,4-dioxin)-poly(styrenesulfonate)
P3HT	Poly(3-hexylthiophene-2,5-diyl) ((C ₁₀ H ₁₄ S) _n)

1. Introduction

1.1. Scope of the paper

Several photovoltaic technologies have now reached the point where they are mature enough, to reach the market and the progress in their power conversion efficiencies are summarized regularly in 'Solar Cell Efficiency Tables' [1]. Crystalline and multi-crystalline Si modules are the industrial standard but amorphous-Si, Cu(In, Ga)(S, Se)₂, CdTe, organic photovoltaic, dye-sensitized solar cells, etc have all been commercialized to varying degrees of success. Whilst these technologies could feasibly cover the majority of photovoltaic applications, increasing the diversity of viable photovoltaic materials will allow for greater adaptability as the technology continues to expand and develop. Additionally, most of the established platforms face challenges related to either the use of critical raw materials, toxic elements, long-term stability, conversion efficiency limitations, cost or low technological flexibility (e.g. incompatibility with flexible substrates, or transparent concepts). These are all important considerations that must be taken into account as the field begins to look towards an era of terawatt level photovoltaic power generation.

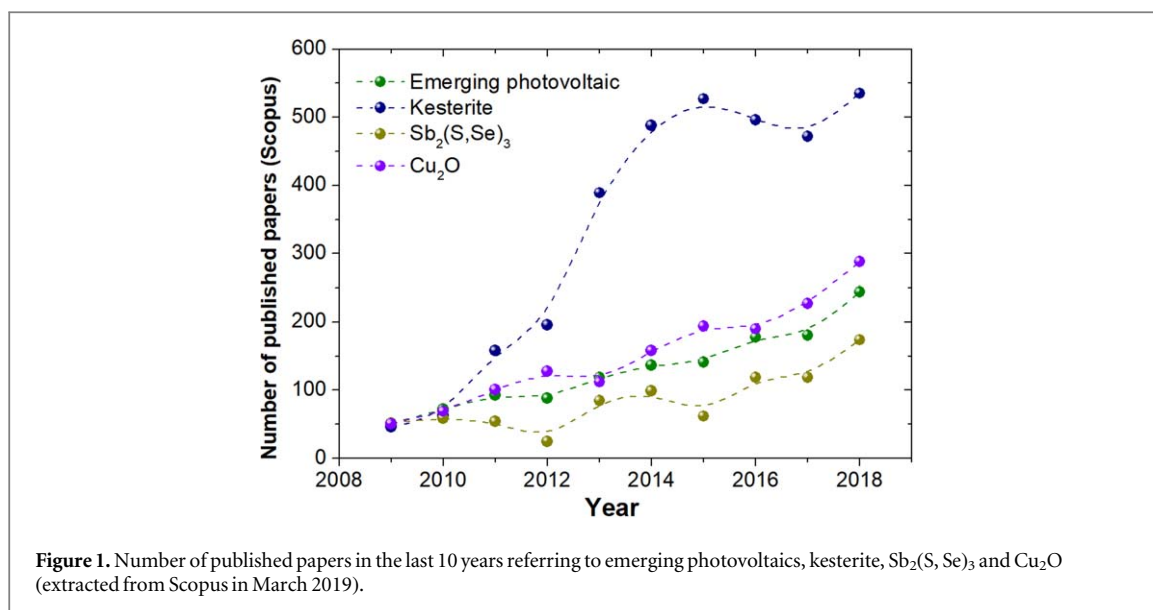
The limitations of the mature technologies encourage a continued search for new materials, as none of the established technologies represent the 'perfect' photovoltaic material. The purpose of continued exploratory research is to identify absorbers that can bring additional benefits and/or may allow the development of novel applications. New inorganic materials including chalcogenides (sulfides, selenides, tellurides), oxides, pnictides (nitrides, phosphides) and halides (mainly bromides and iodides) have proved a fruitful area of research and attracted a lot of attention. There are numerous examples published in recent years showcasing the capability of these materials to act as photovoltaic absorbers. Respectable device efficiencies have been reported for numerous cell platforms despite their typically being only limited attempts at fabrication and often with only specific groups contributing to their progresses. Several of these emerging cell structures have shown enough development to identify them as potential future technological solutions. As a result, there has been a resurgent interest from the scientific community in emerging photovoltaic solar cell absorbers, as is shown in figure 1, where the number of papers published on this topic has increased significantly in the past decade.

Given the continually developing nature of the research field and the large number of emerging inorganic photovoltaic materials, this paper was conceived to collate information on the current status of the most promising materials in form of efficiency tables, collecting and summarizing the most relevant information available in the literature. This includes certified efficiencies in one of the six special centers available in the world, as well as independently measured examples with a description of the means of efficiency verification (or lack thereof). The main aim of these tables is to provide researchers working on emerging inorganic technologies with a valuable information resource by condensing all the spread information about these fascinating materials, but also to establish a forum for the discussion moving forward. It is hoped that these tables will evolve with the field and with input from the researchers in the community, informing future versions to include new champion devices or emerging technologies of note. These tables aim to support and inspire future research in the emerging inorganic solar cells.

1.2. Structure of the paper

The paper is structured in 4 sections, with the following details:

Section 1. is the present section, giving an overview of the paper, a description of its structure, an explanation about the criteria used to select the materials included in the different efficiency tables, and a description of the



recommended procedures for the correct J – V in-house illuminated curve measurement, extraction of corresponding optoelectronic parameters, as well other additional devices information that the authors consider of high relevance for emerging photovoltaic technologies.

Section 2. This section contains the efficiency tables split into two categories. The first table summarizes all the world-class certifications available in the literature, and compiled by the authors. For this table we consider certified devices with efficiency higher than 5% and area larger than 0.1 cm². Exceptions of these considerations are summarized at the end of the table. The second table collects all the devices that are non-certified but can be confirmed using specific procedure, with efficiency higher than 1% and area larger than 0.1 cm². Exceptions of these considerations are also summarized at the end of the table. In each of these two tables, the materials are organized firstly depending on the type of compounds (oxides, chalcogenides, pnictides, halides, etc), and then in terms of complexity from less to more atoms in the structure.

Section 3. In this part of the paper, we give a brief description of new entries in terms of new efficiency records but also new materials included in the tables, with a brief review of the last and most impacting progresses reported in these technologies.

Section 4. The last section of the paper aims to bring to the scientific community a perspective review of a specific topic that the authors have identified as very timely and with high relevance. In this first edition of the efficiency tables, the authors have invited Professor Aron Walsh from Imperial College London, to review the last progresses in predictive modeling of novel materials that are not experimentally demonstrated yet, but have been identified as very promising for their future synthesis and demonstration in the laboratory. Subsequent editions of this yearly published emerging inorganic solar cell efficiency tables will include in this section an invitation of other scientists to review other topics at the forefront of the science.

1.3. Criterion for technology selection

For selecting the materials included in the Efficiency tables, the authors have defined the following criteria:

Table 1 (*World class certification*): fully inorganic technologies with certified materials in one of the six world class certifying centers, with efficiency higher than 5% and area larger than 0.1 cm². Exceptions to these rules are collected separately at the end of the table.

Table 2 (*Non world class certification or in house measurements*): fully inorganic technologies of non-certified materials with efficiency higher than 1%, verification through external quantum efficiency (EQE) measurement, or confirmation by a second organization, and area larger than 0.1 cm². Exceptions to these rules are collected separately at the end of the table.

1.4. General guidelines for efficiency measurement

There are several important documents that define solar cell efficiency measurements, including IEC for general standards and ASTM for Test Methods and Reference Cells. Certification measurements following these

standards are usually performed by one of the internationally recognized institutions, such as NREL (USA), AIST (Japan), JRC (Italy), Fraunhofer ISE (Germany), or a few commercial organizations, and the records are published bi-annually in ‘Solar cell efficiency tables’ for well-established solar cell technologies. However, for the emerging solar cell technologies that are developing very quickly, such certification is not always practical, so only in-house measured PV efficiencies are often reported. Thus, it is important to review here common best practices for in-house solar cell efficiency measurements. The most basic requirements for lab-based solar cell efficiency measurements include:

- (a) Using the Air Mass 1.5 spectrum (AM1.5) for terrestrial cells by choosing the highest-quality solar simulator available.
- (b) Applying one-sun of illumination with intensity of 100 mW cm^{-2} by adjusting the cell/simulator distance to match the expected current of the reference cell.
- (c) Controlling cell temperature during the measurement to $25 \text{ }^\circ\text{C}$ using active cooling or heating.
- (d) Using four-point probe geometry to remove the effect of probe/cell contact resistance.

In addition, there are several other best practices to follow:

- (1) Areas of the measured solar cells have to be carefully defined using device isolation and/or light masking; this is particularly relevant to absorbers with large carrier diffusion lengths.
- (2) Current density–voltage measurements have to be performed in both forward and reverse directions, which is especially important for emerging absorbers with tendency for hysteresis.
- (3) EQE measurement has to be reported, and integrated with the AM1.5 reference spectrum to obtain the current, to be compared to reported J_{sc} .
- (4) Statistical analysis results, including the number of the solar cells measured, and the mean values have to be mentioned.
- (5) Short-time evolution of the reported deficiency has to be verified at the maximum power point or with the photocurrent at maximum power point.
- (6) Long-time stability analysis is encouraged, under light and electrical bias, with measured temperature and humidity.
- (7) For multi-junction solar cells, the illumination bias and voltage bias used for each cell have to be reported.

Finally, we reemphasize that these are just guidelines for in-house solar cell measurements, when external certifications are not practical. However, researchers working on emerging solar cell technologies are strongly encouraged to strive towards perfection and consider submission of their devices to one of the internationally recognized institutions.

2. Efficiency tables

Table 1 presents the list of materials that have been identified by the authors as certified solar cells, and are considered as the highest reported conversion efficiency in their class of technology. The last part of the table collects the technologies that being certified, do not fulfill some of the criteria used for including them in the principal section.

3. New entries

Since this is the first release of the PV Efficiency tables for emerging absorbers, all the entries in tables 1 and 2 can be treated as ‘new’. Therefore, we discuss here only the most important cases and trends observed in the tables, and refer the readers to more details in the original publications.

3.1. Oxides

Oxides represent an important class of emerging inorganic photovoltaic technologies, because of their natural abundance as minerals, and hence their implied low cost and good stability. An archetype oxide PV absorber is cuprous oxide (Cu_2O), which has been studied in the forms of both thin films [7] deposited on the substrate

Table 1. List of certified single-junction record cells under global AM1.5 spectrum (1000 W m^{-2}) at 25°C , including relevant optoelectronic parameters and important additional data (IEC 60904-3: 2008, ASTM G-173-03 global).

Material	Eff. (%)	V_{OC} (V)	J_{SC} (mA cm^{-2})	F. F. (%)	Area (cm^2)	E_g (eV)	Device structure	Certifying Center/ Date	Comments
Sb_2Se_3 (substrate)	9.2	0.400	32.6	70.3	0.26	1.18	Glass/Mo/MoSe ₂ /Sb ₂ Se ₃ /ZnO/AZO	CNIM (2018)	Hebei Key Laboratory of Optic-Electronic Information Materials, Hebei University, China [2]. Substrate geometry structure incorporating core-shell nanowire approach. Absorber deposited by CSS.
$\text{Cu}_2\text{ZnSnS}_4$ (CZTS)	11.0 ± 0.2	0.731	21.74	69.3	0.2339	1.5	Glass/Mo/CZTS/CdS/i-ZnO/ITO/Al/MgF ₂	NREL (2017)	UNSW [3]. Absorber prepared by sputtering Cu/ZnS/SnS
$\text{Cu}_2\text{ZnSn}(\text{S}_{0.25}\text{Se}_{0.75})_4$ (CZTSSe)	12.6 ± 0.3	0.513	35.2	69.8	0.4209	1.13	Glass/Mo/CZTSSe/CdS/ZnO/ITO/Ni/Al/MgF ₂	Newport (2013)	IBM [4]. Absorber prepared by spin-coating a hydrazine-based solution.
$\text{Cu}_2\text{ZnSn}(\text{S}_y\text{Se}_{1-y})_4$ (CZTSSe)	12.62 ± 0.29	0.541	35.35	65.9	0.4804	1.13	Glass/Mo/CZTSSe/CdS/ZnO/AZO/Ni/Al/MgF ₂	Newport (2018)	DGIST [5]. Absorber prepared by sputtering Sn/Cu/Zn and reactive annealing.
$\text{Cu}_2\text{ZnSnSe}_4$ (CZTSe)	11.6	0.423	40.6	67.3	0.43	1.0	Glass/Mo/CZTSe/CdS/ZnO/ITO/Ni/Al/MgF ₂	Newport, (2015)	IBM [6]. Absorber prepared by co-evaporation of Cu, Zn, Sn, and Se.
Notable exceptions									
Cu_2O	3.97 ^a	1.204	7.37	44.70	0.15	2.2	MgF ₂ /Al/Al:ZnO/Ga ₂ O ₃ /Cu ₂ O/Au	NREL (2014)	MIT, Harvard University Cambridge and NREL [7]. Electrochemical deposition.
CsPbI_3	13.58	1.1626	15.246	76.63	0.058	NA	Al/MoO _x /Spiro-OMeTAD/CsPbI ₃ /TiO ₂ /SnO ₂ :F/Glass/MgF ₂	NREL (2017)	NREL, University of Washington and University of Colorado [8]. Coupled quantum dots films.
SnS	4.36 ^a	0.372	20.2	58.0	0.24	1.1	Glass/Mo/SnS/SnO ₂ /Zn(O, S):N/ZnO/ITO	NREL (2014)	Department of Chemistry and Biology, Harvard University, Cambridge, USA [9]. ALD deposition of absorber followed by annealing in H ₂ S.

Table 1. (Continued.)

Material	Eff. (%)	V_{OC} (V)	J_{SC} (mA cm ⁻²)	F. F. (%)	Area (cm ²)	E_g (eV)	Device structure	Certifying Center/ Date	Comments
Sb ₂ Se ₃ (superstrate)	7.6	0.420	29.9	60.4	0.091 ^b	1.18	Glass/ITO/CdS/Sb ₂ Se ₃ /Au	CNIM (2017)	Sargent Joint Research Centre, Wuhan National Laboratory for Optoelectronics and School of Optical and Electronic Information, Huazhong University of Science and Technology, Wuhan, China [10]. Vapor transport deposition.
Sb ₂ (S, Se) ₃	9.9	0.650	24.07	63.5	0.0889	1.53	Glass/FTO/CdS/Sb ₂ Se ₃ /Spiro-OMeTAD/Au	CNIM (2019)	University of Science and Technology of China, China [11]. Hydrothermal method.
PbS	9.88	0.635	21.6	71.9	0.05 ^b	NA	Glass/ITO/ZnO/PbS(TBAI)/PbS(EDT)/Au	Newport (2015)	Wuhan National Laboratory for Optoelectronics and School of Optical and Electronic Information, Huazhong University of Science and Technology, Wuhan, China [12]. Spin coating of PbS colloidal quantum dots.
AgBiS ₂	6.31	0.450	22.1	63.0	0.017 ^b	1.3	Glass/ITO/ZnO/AgBiS ₂ /PTB7/MoO ₃	Newport (2016)	ICFO—Institut de Ciències Fotòniques, The Barcelona Institute of Science and Technology, Barcelona, Spain [13]. Layer-by-layer spin coat deposition from nano-crystal solution.

Note. NA—Not available.

^a Certified efficiency below 5%.

^b Area of the certified cell below 0.1 cm² (total area).

Table 2. List of non-certified single-junction record cells under global AM1.5 spectrum (1000 W m^{-2}) at 25°C , including relevant optoelectronic parameters, the means of verification and important additional data (IEC 60904-3: 2008, ASTM G-173-03 global). ⁺PC-Phtalocyanine.

Material	Eff. (%)	V_{OC} (V)	J_{SC} (mA cm^{-2})	F. F. (%)	Area (cm^2)	E_g (eV)	Device structure	Means of verification	Institutions and Comments
Zn_3P_2	6.0	0.492	14.9	71.0	0.70	NA	ZnS/Mg/Ag: Zn_3P_2 /Ag	No EQE results	<i>U. Delaware</i> [14]. CVT grown thick wafer absorber measured in AMI illumination. Measured under a simulated intensity of 87.5 mW cm^{-2} .
CuSbSe_2	4.7	0.336	26.3	53.0	0.2	NA	Glass/Mo/ CuSbSe_2 /ZnO/AZO	EQE, In-house	<i>National Renewable Energy Laboratory, Golden, USA</i> [15]. Sputtering from binary Cu_2Se and Sb_2Se_3 targets.
CuSbS_2	3.2	0.470	15.6	43.6	0.45	1.4–1.9	Glass/Mo/ CuSbS_2 /CdS/ZnO/AZO	EQE, In-house	New and Renewable Energy Research Division, Korea Institute of Energy Research, Daejeon, South Korea [16]. Sulfurization of nanoparticle inks.
$\text{Cu}_2\text{CdSnS}_4$	1.1	0.383	12.4	23.0	0.16	1.41	Glass/Mo/CCdTS/CdS/ZnO/AZO/Ag	EQE, In-house	<i>NTU</i> [17]. Absorber prepared by spin-coating using 2-methoxyethanol-based solution
$\text{Cu}_2\text{ZnSnSe}_4$	11.8	0.463	38.3	66.3	0.522	1.05	Glass/Mo/CZTSe/CdS/ZnO/ITO/Ag/MgF ₂	EQE, in-house, measured in two centers	<i>IREC, Spain; AIST, Japan; University of Barcelona, Spain; Martin-Luther-Universitat Halle-Wittenberg, Germany</i> [18]. Sputtering of metallic precursors and reactive annealing. Ge doping (less than 0.5%).
$\text{Cu}_2\text{BaSnS}_4$ (substrate)	1.7	0.698	5.3	46.9	0.2	2.01	Glass/Mo/CBaTS/CdS/ZnO/ITO/Al	EQE, In-house	<i>Central South University, UNSW, Shen Zhen University, Xiamen University</i> [19]. Absorber prepared by spin-coating using a 2-methoxyethanol-based solution.
$\text{Cu}_2\text{BaSnS}_4$ (superstrate)	2.0	0.933	5.1	42.9	0.2	2.04	CdS:O/CdS/ZnO/AZO	EQE, In-house	<i>The University of Toledo</i> [20]. Absorber prepared by sputtering method.
$\text{Cu}_2\text{FeSnS}_4$	3.0	0.610	9.3	52.0	0.1	1.5	ITO/Cu-NiO/CFeTS/ Bi_2S_3 /ZnO/Al	EQE, In-house	Indian Association for the Cultivation of Science [21]. Absorber prepared by SILAR method.
$\text{Cu}_2\text{CdSn}(\text{S}_{0.xx}\text{Se}_{0.yy})_4$	2.8	0.356	18.8	41.6	0.405	1.55	Glass/Mo/CCdTSSe/CdS/ZnO/ITO/Al	EQE, In-house	<i>Changchun Institute of Applied Chemistry, Chinese Academy of Sciences</i> [22]. Absorber prepared by spin-coating an ethanol, butyldithiocarbamic acid, and thioglycolic acid -based solution.

Table 2. (Continued.)

Material	Eff. (%)	V_{OC} (V)	J_{SC} (mA cm^{-2})	F. F. (%)	Area (cm^2)	E_g (eV)	Device structure	Means of verification	Institutions and Comments
$\text{Cu}_2\text{BaSn}(\text{S}_{0.9x}\text{Se}_{0.1y})_4$	5.2	0.611	17.4	48.9	0.425	1.55	Glass/Mo/CBaTSSe/CdS/ZnO/ITO/Ni/Al	EQE, In-house	Duke University, IBM [23]. Absorber prepared by co-sputtering using Cu, Sn, and BaS.
$\text{Cu}_2\text{ZnGe}(\text{S}_{0.9x}\text{Se}_{0.1y})_4$	6.0	0.617	NA	NA	0.25	1.47	Glass/Mo/CZGeSSe/CdS/ZnO/AZO/Ni/Al	EQE, In-house	ZSW, CNRS [24]. Absorber prepared by doctor-blade coating a DMF-based solution.
$\text{Cu}_2\text{ZnGeSe}_4$	7.6	0.558	22.8	59.0	0.5	1.36	Glass/Na-barrier/Mo/CZGeSe/CdS/ZnO/AZO/Ni/Al	EQE, In-house	CNRS, IMEC [25]. Absorber prepared by sputtering of Cu and Zn, and e-beam evaporation of Ge.
$\text{Ag}_2\text{ZnSnSe}_4$	5.18	0.504	21.0	48.7	0.45	1.35	FTO/AgZTSe/MoO ₃ /ITO/Ni/Al	EQE, In-house	IBM, UCSD [26]. Absorber prepared by co-evaporation of Ag, Zn, Sn, and cracked Se.
$\text{Cu}_2(\text{Zn}_{0.6}\text{Cd}_{0.4})\text{SnS}_4$	11.0	0.650	25.5	66.1	0.22	1.38	Glass/Mo/CZCdTS/CdS/ZnO/ITO/Al/MgF ₂	EQE, in-house	University of New South Wales, Australia; National Renewable Energy Laboratory, United States; Central South University, China [27]. Sulfurized chemical bath deposited CdS on top of co-sputtered Cu/ZnS/SnS precursor.
$(\text{Ag}_{0.05-0.3}\text{Cu}_{0.95-0.7})_2\text{ZnSn}(\text{S}, \text{Se})_4$	11.2	0.464	36.2	66.5	0.21	Graded	Glass/Mo/ACZTSSe/CdS/ZnO/ITO/Ag	EQE, in-house	Henan University, China [28]. Spin coating of ethanol based solutions.
$(\text{Ag}_{0.05}\text{Cu}_{0.95})_2(\text{Zn}_{0.75}\text{Cd}_{0.25})\text{Sn}_4$	10.1	0.650	23.4	66.2	0.16	1.4	Glass/Mo/ACCdZTS/CdS/ITO/Ag	EQE, in-house	NTU, Singapore; HZB, Germany [29]. Spin coating of 2-methoxyethanol based solution.
$\text{Cu}_2\text{Zn}(\text{Sn}_{0.78}\text{Ge}_{0.22})\text{Se}_4$	12.3	0.527	32.2	72.7	0.519	1.11	Glass/Mo/CZTGTSe/CdS/ZnO/AZO/Ag/ARC	EQE, in-house	AIST, Japan [30]. Co-evaporation and reactive annealing.
$(\text{Li}_{0.06}\text{Cu}_{0.94})_2\text{ZnSn}(\text{S}, \text{Se})_4$	11.6	0.531	33.7	64.8	0.285	1.13	Glass/SiO _x /Mo/LiCZTSSe/CdS/ZnO/AZO/Ni/Al/MgF ₂	EQE, in-house	EMPA, Switzerland; Universidad Autónoma de Madrid, Spain; HZB, Germany [31]. Spin coating of DMSO based solution.
$\text{Cu}_2(\text{Zn}_{0.95}\text{Mn}_{0.05})\text{Sn}(\text{S}, \text{Se})_4$	8.9	0.418	33.7	63.3	0.34	1.06	Glass/Mo/CMZTSSe/CdS/ZnO/AZO/Ni/Al	EQE	Nankai University, China; National Institute of Material Science, Japan [32]. Spin coating of 2-methoxyethanol based solution.
Notable exceptions									
Cu_2O	8.1	1.2	10.4	65.0	0.03 ^a	2.2	MgF ₂ /Al:ZnO/Zn _{0.38} Ge _{0.62} O/Cu ₂ O:Na/Au	No EQE results	Kanazawa I. T. [33]. Cu ₂ O sheets oxidized from Cu foils.

Table 2. (Continued.)

Material	Eff. (%)	V_{OC} (V)	J_{SC} (mA cm^{-2})	F. F. (%)	Area (cm^2)	E_g (eV)	Device structure	Means of verification	Institutions and Comments
$\text{Bi}_2\text{FeCrO}_6$	8.1	0.84	20.6	46.0	NA ^a	1.4	$\text{Sn:In}_2\text{O}_3/\text{Bi}_2\text{FeCrO}_6/\text{SrRuO}_3$	EQE, In-house	INRS Canada [34]. PLD absorber with three-layer stack.
InP	7.3	0.57	17.4	73.0	0.0625 ^a	1.32	$\text{Al/ZnO:Al/i-ZnO/InP:Zn/Au-Zn-Au}$	EQE, In-house	Purdue U., The U. of California, and The Pennsylvania State U [35]. Pulsed laser deposition.
(In, Ga)N	3.0	1.8	2.6	64.0	0.046 ^a	NA	$\text{SiO}_2/\text{Au}/(\text{Mg:GaIn}/\text{GaIn})/(\text{In, Ga})\text{N}/\text{Si:GaIn}$	No EQE results	Texas Tech. [36]. MOCVD MQW absorber.
ZnSnN_2	1.5	0.36	7.5	57.0	0.06 ^a	1.4	$\text{Au/ZnSnN}_2/\text{Al}_2\text{O}_3/\text{SnO}$	No EQE results	Ningbo, China [37]. Sputtered absorber.
BiI_3	1.2	0.607	5.3	37.6	0.04 ^a	1.72	$\text{Au/F8/BiI}_3/\text{TiO}_2/\text{SnO}_2:\text{F}^b$	EQE, In-house	U. Bristol [38]. Spin coating of $\text{Bi}(\text{NO}_3)_3$ and thiourea, followed by thermolysis at 200 °C to produce a homogeneous Bi_2S_3 film that is subsequently iodinated upon exposure to the I_2 gas.
CsPbBr_3	8.8	1.310	8.2	81.4	0.071 ^a	2.32	$\text{C}/\text{CuPc}^+/\text{CsPbBr}_3/\text{SnO}_2/\text{TiO}_2/\text{SnO}_2:\text{F}^b$	EQE, In-house	Huazhong U. Science and Technology [39]. Multi-step solution process method.
CsPbI_3	15.7	1.08	18.4	79.3	0.108	1.73	$\text{Au}/\text{Spiro-OMeTAD}/\text{CsPbI}_3/\text{SnO}_2/\text{In}_2\text{O}_3:\text{SnO}_2^b$	EQE, In-house	Chinese Academy of Science [40]. Spin coating and soft annealing.
CsPbI_2Br	16.1	1.23	16.8	77.8	0.1	N. R.	$\text{Au}/\text{Spiro-OMeTAD}/\text{CsPbI}_2\text{Br}/\text{TiO}_2/\text{In}_2\text{O}_3:\text{SnO}_2^b$	EQE, In-house	Soochow University and Chinese Academy of Science [41]. Spin coating.
CsPbIBr_2	9.2	1.245	10.7	69.0	0.09 ^a	2.05	$\text{C}/\text{CsPbIBr}_2/\text{TiO}_2/\text{SnO}_2:\text{F}$	EQE, In-house	Xidian U [42]. Precursor solution by spin coating. The JV curves present hysteresis.
$\text{CsPb}_{0.95}\text{Eu}_{0.05}\text{I}_2\text{Br}$	13.7	1.22	14.6	76.6	0.16	1.92	$\text{Au}/\text{Spiro-OMeTAD}/\text{CsPb}_{0.95}\text{Eu}_{0.05}\text{I}_2\text{Br}/\text{TiO}_2/\text{SnO}_2:\text{F}^b$	EQE, In-house	Wuhan U. Technology, EPFL, Nankai U [43]. Precursor solution by spin coating. Some hysteresis is observed.
CsSnBr_3	2.2	0.42	9.1	57.0	NA ^a	1.75	$\text{Au}/\text{Spiro-OMeTAD}/\text{CsSnBr}_3/\text{TiO}_2/\text{SnO}_2:\text{F}^b$	EQE, In-house	Weizmann Institute of Science [44]. Spin coating. The EQE integration gives 2 mA cm^{-2} less current density.
CsSnI_3	4.8	0.382	25.7	49.1	~ 0.15	1.30	$\text{Au}/\text{PTAA}/\text{CsSnI}_3/\text{TiO}_2/\text{SnO}_2:\text{F}^b$	EQE, In-house	Northwestern University and Mitsubishi Chemical Group Science & Technology Research Center [45]. Spin coating with hydrazine. Integrated EQE gives J_{sc} of approximately 24 mA cm^{-2} .

Table 2. (Continued.)

Material	Eff. (%)	V_{OC} (V)	J_{SC} (mA cm^{-2})	F. F. (%)	Area (cm^2)	E_g (eV)	Device structure	Means of verification	Institutions and Comments
$\text{CsSn}_{0.5}\text{Ge}_{0.5}\text{I}_3$	7.1	0.63	18.6	60.6	0.1	1.50	Au/Spiro-OMeTAD/ $\text{CsSn}_{0.5}\text{Ge}_{0.5}\text{I}_3$ /PCBM/ SnO_2 :F ^b	EQE, In-house	Brown U, U. of Nebraska-Lincoln, Worcester Polytechnic Institute, and Okinawa Institute of Science and Technology Graduate University [46]. Powder synthesized by solid-state reaction and thermally evaporated.
Se	6.5	0.969	10.6	63.4	0.027 ^a	1.95	Glass/FTO/ TiO_2 /ZnMgO/Se/ MoO_3 /Au	EQE, In-house	IBM Thomas J. Watson Research Center, Yorktown Heights, USA [47]. GeSe thermal evaporation of Se at room temperature followed by post-deposition annealing.
GeSe	1.5	0.240	14.5	42.6	0.09 ^a	1.1–1.2	Glass/ITO/CdS/GeSe/Au	EQE, In-house	Beijing National Laboratory for Molecular Sciences, Key Laboratory of Molecular Nanotechnology and Nanotechnology, Institute of Chemistry, Beijing, China [48]. Rapid thermal sublimation.
Sb_2S_3	7.5	0.711	16.1	65.0	0.16	1.7	Glass/FTO/ TiO_2 /mp- TiO_2 / Sb_2S_3 /PCPDTBT/PEDOT:PSS/Au ^b	EQE, In-house	Division of Advanced Materials, Korea Institute of Chemical Technology, Daejeon, Republic of Korea [49]. Chemical bath deposition followed by additional sulfurization.
$\text{Sb}_2(\text{S}_x\text{Se}_{1-x})_3$	6.6	0.475	24.9	55.6	0.12	1.3–1.7	Glass/FTO/ TiO_2 /mp- TiO_2 / Sb_2S_3 /P3HT/Au ^b	EQE, In-house	Division of Advanced Materials, Korea Institute of Chemical Technology, Daejeon, Republic of Korea [50]. Combination of spin coating and chemical bath deposition.
Bi_2S_3	3.3	0.700	10.7	45.0	0.18	1.2	Glass/ITO/P3HT: Bi_2S_3 / MoO_x /Au ^b	EQE, In-house	Department of Chemical and Biological Engineering, Princeton University, USA [51]. Percolated Bi_2S_3 network with P3HT.
$\text{Cu}_2\text{CdGeSe}_4$	4.2	0.464	23.3	39.0	0.02 ^a	1.27	Graphite/Epoxy/CCdGeSe/ CdS / ZnO /AZO/glue/Ag/glass	EQE, In-house	Tallinn University of Technology [52]. Absorber prepared by molten salt method using CdI_2 and KI as fluxes. Monograin-based device.

Note. NA—Not available.

^a Area of the non-certified cell below 0.1 cm^2 or not reported.

^b Devices includes at least one organic carriers transport layer.

(certified 3.97% efficiency, table 1) and thick sheets oxidized from Cu foils (non-certified 8.1% efficiency, table 2) [33]. In both cases, a V_{oc} of 1.2 V was achieved, which is remarkable compared to other emerging PV technologies, albeit for the Cu_2O material with 2.1 eV band gap. The major advance that led to both of these records was the design of new n-type window layer for p-type Cu_2O -based heterojunction solar cells, $Zn_{1-x}Ge_xO$ by pulsed laser deposition in the case of the Cu_2O thick foils, and Ga_2O_3 by atomic layer deposition in the case of the Cu_2O thin films.

Another curious class of emerging oxide PV absorbers is exemplified by Bi_2FeCrO_6 with perovskite-derived crystal structure and multiferroic properties. In one high-profile report it was shown that the Bi_2FeCrO_6 based thin films solar cells with multilayer configuration can reach the non-certified efficiency of 8.1% (table 2) [34], and that the JV curve polarity can be reversed by applying external electric field. Furthermore, it was argued that such non-centrosymmetric materials can 'lead to energy conversion efficiencies beyond the maximum value ($\sim 34\%$)' [34]. Another high-profile study claimed 'power conversion efficiency exceeding the Shockley–Queisser limit in a ferroelectric insulator' [53], and provided some experimental data for the related $BaTiO_3$ perovskite. Overall, it appears that certification of such unusual devices, or at least a cross-lab validation study between different groups working on this topic [34, 53], would significantly move forward this curious emerging PV technology.

3.2. Chalcogenides

Chalcogenide represents an important family of inorganic semiconductor materials for the development of photovoltaic absorber materials. It probably has the longest history with the first chalcogenide Se solar cells dated back to 1876 [54]. Chalcogenides absorber materials range from single elemental (Se), to binary (CdTe, PbS, SnS, $Sb_2(S, Se)_3$) and to multinary compounds ($Cu(In, Ga)(S, Se)_2$ (CIGS) and $Cu_2ZnSn(S, Se)_4$ (CZTSSe)). In recent decades, the power conversion efficiency of chalcogenides based solar cells has witnessed an unprecedented increase and successful deployment at the industrial scale. The certified efficiency of $>22\%$ achieved by CdTe and $Cu(In, Ga)Se_2$ are already on par with the most mature traditional silicon wafer solar cells. In addition to the high efficiency and successful commercialization achieved with the chalcogenides, recent decades also witnessed the progress of emerging chalcogenide materials, particularly those with earth-abundant, non-toxic/less toxic constituents (such as kesterites and $Sb_2(S, Se)_3$).

Kesterite, derived from CIGS, is one of the most promising emerging chalcogenides. Certified efficiency of $>10\%$ has been demonstrated for high bandgap pure sulfide CZTS (11%) by UNSW [3], low bandgap pure selenide kesterites CZTSe (11.5%) by IBM [6], with the champion efficiency of 12.6% for kesterite CZTSSe by IBM and DGIST [4, 5]. The reason behind the large gap between the record efficiency and the Shockley–Queisser limit ($\sim 30\%$) is still debatable but it is generally agreed that reducing the point defects (such as Cu/Zn, Zn/Sn and Cu/Sn antisites) would enhance the optoelectronic properties of kesterites. Most recent work explored cation substitution to reduce point defects and to realize the band-grading of kesterites inspired by the successful approaches of CIGS and CdTe. Partial substitutions of Cu by Ag, Zn by Cd and Ba show positive effects in reducing harmful defects and lead to improved optoelectrical properties [17, 19, 26]. Partial substitution of Sn by Ge and Cu by Ag were demonstrated successfully in tuning the kesterites bandgap and even realizing the band grading [24–26, 28]. So far around 10% efficiency kesterite devices have been demonstrated for Ag-, Cd- and Ge-alloyed CZTS(Se) [17, 27, 28]. Additionally, working devices with large range of bandgap (from 1.0 to 2 eV) were fabricated [6, 19]. Although some of these alloyed/doped kesterites showed reasonably high efficiencies (some with in-house measured active area efficiency $>10\%$), the champion efficiency is still held by the nominally 'undoped/unalloyed' kesterites. The understanding of dopant/alloying element induced changes particularly in the point defects and associated interface engineering would lead to further performance improvement. For a more complete review of the recent approaches of cation substitution in kesterites, readers may refer to the review article by Giraldo *et al* [55].

Another group of emerging chalcogenides showing greatly increased efficiency in recent years is Sb-based chalcogenides. Whilst work on improving the Cu–Sb–S/Se ternaries has proved frustratingly slow, the binary Sb_2Se_3 and Sb_2S_3 materials have shown consistent progress. These materials are of particular note as they are one-dimensional materials with highly anisotropic optical, electrical and structural properties [56]. The selenide variants are currently leading in this class with majority of work having focussed on the CdTe-style superstrate planar configuration, yielding efficiencies of up to 7.6% [10] for Sb_2Se_3 and 9.9% for $Sb_2(S, Se)_3$, certified but not published yet [57]. Recently though an inverted substrate configuration which also incorporates core–shell style structures has yielded 9.2% efficiency [2]. This emphasizes that vast amounts are still unknown about this technology even extending to whether superstrate or substrate approaches are optimal. Developing routes to consistently obtaining desired $[hkl]$ crystalline orientations, surface/defect passivation treatments and the determination of optimal heterojunction partner layers are the key steps to realizing further efficiency improvements [56, 58].

3.3. Pnictides

There are no certified pnictide (nitride, phosphide) emerging PV technologies. An archetype example of emerging phosphide absorbers are Zn_3P_2 wafers [14], which have shown non-certified efficiencies of 6.0% (table 2). More recent work reported on Mg/ZnS/ Zn_3P_2 metal–insulator–semiconductor solar cells with Zn_3P_2 thin films grown by molecular beam epitaxy has demonstrated 1.4% efficiency [59]. The emerging PV nitride absorbers are represented by ZnSnN_2 , which was only discovered a few years ago. This emerging absorber material has been recently reported by one group to have up to 1.5% efficiency in sputtered form [37, 60]. Another interesting case is (In, Ga)N with multiple quantum wells grown by metal organic chemical vapor deposition, also used in light emitting diodes. Such emerging absorbers have been reported to have 3%–4% energy conversion efficiencies with remarkable V_{oc} of 1.8–1.9 V by several groups [36, 61].

3.4. Halides

Inorganic halides have gained a lot of interest after the very fast progress of hybrid organic–inorganic lead halide perovskites. Simple compounds (binary metal halides) have been very marginally studied, and the most notable case is the recently reported solar cell based on BiI_3 , using a simple device structure [38]. Most of the works currently available in the literature are centered in the development of inorganic cesium–lead–halide perovskites, mainly the bromide, iodide and mixed compounds. Starting with the pioneer works of Kulbak *et al* in CsPbBr_3 [62], Eperon *et al* in CsPbI_3 [63], and Ma *et al* in CsPbIBr_2 [64], the conversion efficiency of this system has notably increased in the last 2 years, and the current record (not world-class certified) is 16.07% [41]. These materials exhibit excellent properties as photovoltaic absorbers, including very high electron and holes mobility ($2300 \text{ cm}^2 \text{ V s}^{-1}$ for electrons and $320 \text{ cm}^2 \text{ V s}^{-1}$ for holes) [64], and lifetimes in the 5–50 ns range [39, 64, 65].

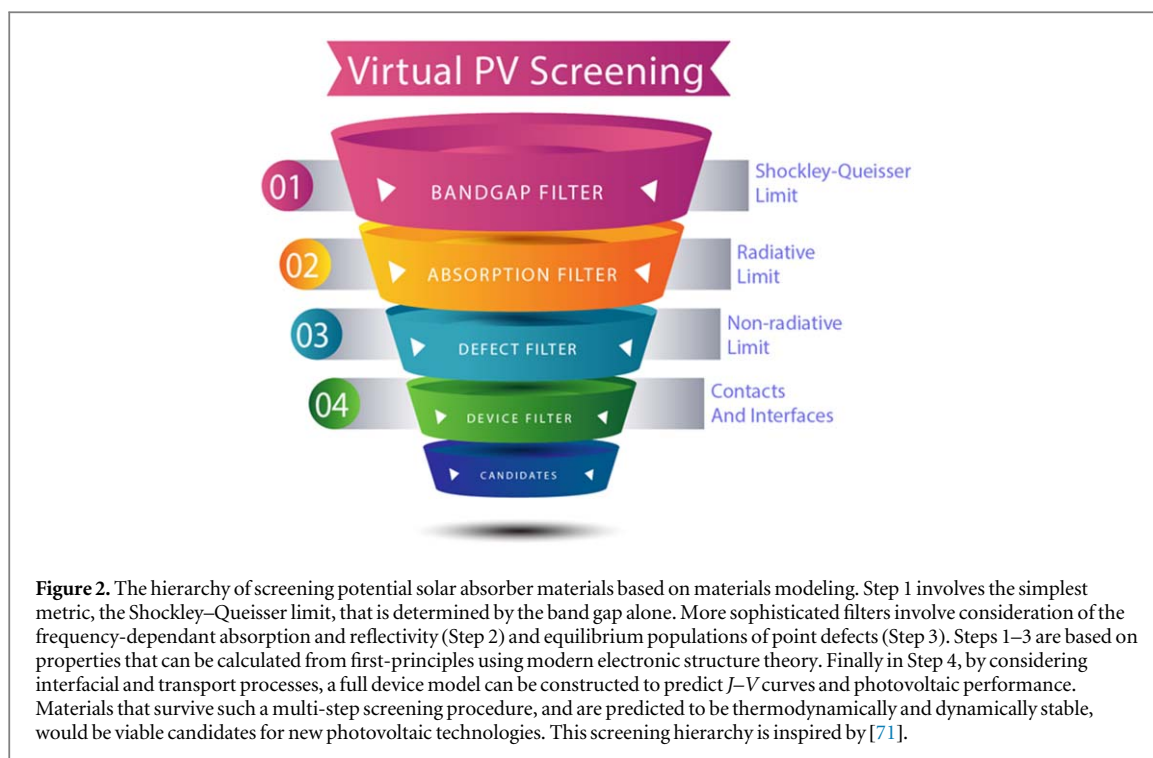
Partial substitution of Pb by Eu (~5%, $\text{CsPb}_{0.95}\text{Eu}_{0.05}\text{I}_2\text{Br}$) has shown also a positive effect on the solar cell devices performance, boosting the efficiency from 10.2% without Eu up to 13.7% with 5% Eu [43], and leading to a large increase in the electrons lifetime, but also improved stability. Last trend in this topic is related to the substitution of Pb by less toxic elements, where the most rational candidate is Sn. First attempts reporting devices with full substitution of Pb by Sn, demonstrated efficiencies in the 2%–5% range approximately [44, 45]. Main challenge of these materials is the multi-valence of Sn, which can easily adopt (II) and (IV) oxidation states. This has been at least partially solved by introducing Ge in the structure, increasing the record efficiency up to 7.11% for a compound with the formula $\text{CsSn}_{0.5}\text{Ge}_{0.5}\text{I}_3$ [46].

4. Latest progresses in selected topic: modeling of emerging PV materials

First-principles materials modeling has become increasingly predictive when it comes to the properties of semiconductors [66]. Beyond the electronic properties of bulk crystals (e.g. chemical bonding and band gap), the thermodynamic stability (phase diagrams), and optical properties (frequency-dependant absorption coefficient) are now accessible through routine calculation procedures. Currently, large computational materials databases such as Materials Project (<https://materialsproject.org>) [67] are based on a level of theory (semi-local density functional theory) that results in unreliable band gaps. This makes them unsuitable for screening studies or for training machine learning models for solar energy conversion.

A second factor currently limiting large-scale computational searches is the lack of a simple efficiency metric such as the case of ZT for thermoelectric devices (where ZT is a figure of merit used for thermoelectric devices, and $ZT = S^2T/\rho\kappa$, with S the Seebeck coefficient, T the absolute temperature, ρ the electrical resistivity, and κ the thermal conductivity). Searches based on band gaps alone are simplistic, and have been surpassed by approaches that take into account the integrated optical absorption such as the spectroscopically-limited maximum efficiency (SLME) [68]. In their screening of chalcopyrite materials, Yu and Zunger identified 25 high-efficiency candidates including known systems like CuInS_2 to more adventurous predictions such as CuBSe_2 and Cs_3AlTe_3 . The SLME metric has also been applied to the $\text{PbS–Bi}_2\text{S}_3$ series, where PbBi_2S_4 emerged as an earth-abundant absorber layer, with a predicted maximum efficiency of 26% at a film thickness of $0.2 \mu\text{m}$ [69]. Consideration of Zn-based metal nitride semiconductors highlighted the potential of LiZnN , KZnN , CaZn_2N_2 , Sr_2ZnN_2 , Ba_2ZnN_2 , Zn_3LaN_3 and ZnSnN_2 [70].

More sophisticated simulation procedures can take into account detailed balance analysis, with consideration of factors including carrier mobility and lifetimes (see figure 2) [71]. Indeed minority carrier lifetime is often the bottleneck for emerging technologies, which manifests as large open-circuit voltage deficits. For this reason, the majority of materials modeling of photovoltaic materials is focused on identifying defects that can give rise to non-radiative recombination [72]. While in the past, only the position of the defect levels in the band gap were accessible, recent progress has made prediction of carrier capture and recombination rates possible from first-principles [73]. In this way the most detrimental defects can be identified, for example Sn_{Zn}



and V_S are predicted to act as giant carrier traps in $\text{Cu}_2\text{ZnSnS}_4$ [74]. However, such calculations are challenging in terms of human effort and calculation time so they have been performed for very few systems.

Progress in this field is rapid with ongoing explorations of metal oxide, chalcogenide, pnictide and halide semiconductors, as well as their mixtures. Materials modeling is already established as an essential tool in the characterization and optimization of photovoltaic materials and processes; however, with further development it has the potential to deliver greater impact by directing researchers to the promising classes of materials that have yet to emerge.

Acknowledgments

ES thanks H2020 EU Programme under the projects STARCELL (H2020-NMBP-03-2016-720907) and INFINITE-CELL (H2020-MSCA-RISE-2017-777968), the Spanish Ministry of Science, Innovation and Universities for the IGNITE project (ENE2017-87671-C3-1-R), and the European Regional Development Funds (ERDF, FEDER Programa Competitivitat de Catalunya 2007–2013). IREC belong to the SEMS (Solar Energy Materials and Systems) Consolidated Research Group of the ‘Generalitat de Catalunya’ (Ref 2017 SGR 862). AW is supported by a Royal Society University Research Fellowship. JDM is supported by an EPSRC Early Career Fellowship (EP/N014057/1). LHW thanks Shreyash Hadke for compiling the selected literature for complex chalcogenides and acknowledges funding from CREATE Programme under the Campus for Research Excellence and Technological Enterprise (CREATE), which is supported by the National Research Foundation, Prime Minister’s Office, Singapore; and Ministry of Education (MOE) Tier 2 Project (MOE2016-T2-1-030). AZ was supported by the US Department of Energy (DOE) under Contract No. DEAC36-08GO28308 with the Alliance for Sustainable Energy, LLC, the manager and operator of the National Renewable Energy Laboratory (NREL), with the funding provided by the Office of Energy Efficiency and Renewable Energy (EERE), Solar Energy Technologies Program (SETP). AZ would like to thank Dean Levi at NREL for useful discussions. XH thanks Australian Renewable Energy Agency (ARENA) for the projects 1-USO028 and RND004 and Australian Research Council (ARC) for the project LP150100911.

Disclaimer

The information presented in this review was selected in good faith by all the authors. Errors and omissions will be corrected in the subsequent editions of the Table. Corrections and more complete information from the scientific community are most welcome in order to improve the accuracy of the values presented in the Efficiency Tables.

Authors description and contribution

Professor Lydia H Wong, contributed to compile the information about complex chalcogenides (4 atoms or more), and to write section 3.2. **Dr Andriy Zakutayev**, contributed to compile the information about oxides and pnictides, and to write sections 1.4, 3.1 and 3.3. **Dr Jonathan D Major**, contributed to compile the information about simple chalcogenides (3 atoms or less), and to write section 3.2. **Associate Professor Xiaojing Hao**, contributed to compile the information about complex chalcogenides (3 atoms or more), and to write section 3.2. **Professor Aron Walsh**, contributed to write section 4. **Dr Teodor K Todorov**, contributed to compile the information about simple chalcogenides (3 atoms or less), and to write section 3.2. **Dr Edgardo Saucedo**, acted as leader and corresponding author of the paper. He contributed to compile the information about halides and build the complete version of the Efficiency Tables, and to write sections 1.1–1.3, and 3.4.

All the authors contributed equally to define the structure and content of the manuscript, to the general review and final approval of the paper.

ORCID iDs

Lydia H Wong  <https://orcid.org/0000-0001-9059-1745>

Andriy Zakutayev  <https://orcid.org/0000-0002-3054-5525>

Jonathan D Major  <https://orcid.org/0000-0002-5554-1985>

Xiaojing Hao  <https://orcid.org/0000-0001-5903-4481>

Aron Walsh  <https://orcid.org/0000-0001-5460-7033>

Edgardo Saucedo  <https://orcid.org/0000-0003-2123-6162>

References

- [1] Green M A, Hishikawa Y, Dunlop E D, Levi D H, Hohl-Ebinger J, Yoshita M and Ho-Baillie A W Y 2019 *Prog. Photovoltaics Res. Appl.* **27** 3
- [2] Li Z et al 2019 *Nat. Commun.* **10** 125
- [3] Yan C et al 2018 *Nat. Energy* **3** 764
- [4] Wang W, Winkler M T, Gunawan O, Gokmen T, Todorov T K, Zhu Y and Mitzi D B 2014 *Adv. Energy Mater.* **4** 1301465
- [5] DGIST 2019 private communication
- [6] Lee Y S, Gershon T, Gunawan O, Todorov T K, Gokmen T, Virgus Y and Guha S 2015 *Adv. Energy Mater.* **5** 1401372
- [7] Lee Y S, Chua D, Brandt R E, Siah S C, Li J V, Mailoa J P, Lee S W, Gordon R G and Buonassisi T 2014 *Adv. Mater.* **26** 4704
- [8] Sanhira E M, Marshall A R, Christians J A, Harvey S P, Ciesielski P N, Wheeler L M, Schulz P, Lin L Y, Beard M C and Luther J M 2017 *Sci. Adv.* **3** eaao4204
- [9] Sinsersuksakul P, Sun L, Lee S W, Park H H, Kim S B, Yang C and Gordon R G 2014 *Adv. Energy Mater.* **4** 1400496
- [10] Wen X et al 2018 *Nat. Commun.* **9** 2179
- [11] Wu C, Zhang L, Ding H, Ju H, Jin X, Wang X, Zhu C and Chen T 2018 *Sol. Energy Mater. Sol. Cells* **183** 52
- [12] Yang X et al 2017 *Nano-Micro Lett.* **9** 24
- [13] Bernechea M, Miller N C, Xercavins G, So D, Stavrinadis A and Konstantatos G 2016 *Nat. Photon.* **10** 521
- [14] Bhushan M and Catalano A 1981 *Appl. Phys. Lett.* **38** 39
- [15] Welch A W, Baranowski L L, Peng H, Hempel H, Eichberger R, Unold T, Lany S, Wolden C and Zakutayev A 2017 *Adv. Energy Mater.* **7** 1601935
- [16] Banu S, Ahn S J, Ahn S K, Yoon K and Cho A 2016 *Sol. Energy Mater. Sol. Cells* **151** 14
- [17] Su Z, Tan J M R, Li X, Zeng X, Batabyal S K and Wong L H 2015 *Adv. Energy Mater.* **5** 1500682
- [18] Giraldo S et al 2018 *Energy Environ. Sci.* **11** 582
- [19] Chen Z, Sun K, Su Z, Liu F, Tang D, Xiao H, Shi L, Jiang L, Hao X and Lai Y 2018 *ACS Appl. Energy Mater.* **1** 3420
- [20] Ge J, Koirala P, Grice C R, Roland P J, Yu Y, Tan X, Ellingson R J, Collins R W and Yan Y 2017 *Adv. Energy Mater.* **7** 1601803
- [21] Chatterjee S and Pal A J 2017 *Sol. Energy Mater. Sol. Cells* **160** 233
- [22] Zhao W, Wang G, Tian Q, Huang L, Gao S and Pan D 2015 *Sol. Energy Mater. Sol. Cells* **133** 15
- [23] Shin D, Zhu T, Huang X, Gunawan O, Blum V and Mitzi D B 2017 *Adv. Mater.* **29** 1606945
- [24] Schnabel T, Seboui M, Bauer A, Choubrac L, Arzel L, Harel S, Barreau N and Ahlswede E 2017 *RSC Adv.* **7** 40105
- [25] Choubrac L, Brammertz G, Barreau N, Arzel L, Harel S, Meuris M and Vermang B 2018 *Phys. Status Solidi* **215** 1800043
- [26] Gershon T, Sardashti K, Gunawan O, Mankad R, Singh S, Lee Y S, Ott J A, Kummel A and Haight R 2016 *Adv. Energy Mater.* **6** 1601182
- [27] Yan C et al 2017 *ACS Energy Lett.* **2** 930
- [28] Qi Y-F, Kou D-X, Zhou W-H, Zhou Z-J, Tian Q-W, Meng Y-N, Liu X-S, Du Z-L and Wu S-X 2017 *Energy Environ. Sci.* **10** 2401
- [29] Hadke S H, Levchenko S, Lie S, Hages C J, Márquez J A, Unold T and Wong L H 2018 *Adv. Energy Mater.* **8** 1802540
- [30] Kim S, Kim K M, Tampo H, Shibata H and Niki S 2016 *Appl. Phys. Express* **9** 102301
- [31] Cabas-Vidani A et al 2018 *Adv. Energy Mater.* **8** 1801191
- [32] Li X, Hou Z, Gao S, Zeng Y, Ao J, Zhou Z, Da B, Liu W, Sun Y and Zhang Y 2018 *Sol. RRL* **2** 1800198
- [33] Minami T, Nishi Y and Miyata T 2013 *Appl. Phys. Express* **6** 044101
- [34] Nechache R, Harnagea C, Li S, Cardenas L, Huang W, Chakrabarty J and Rosei F 2015 *Nat. Photon.* **9** 61
- [35] Nian Q, Montgomery K H, Zhao X, Jackson T, Woodall J M and Cheng G J 2015 *Appl. Phys. A* **121** 1219
- [36] Dahal R, Li J, Aryal K, Lin J Y and Jiang H X 2010 *Appl. Phys. Lett.* **97** 073115
- [37] Javaid K, Wu W, Wang J, Fang J, Zhang H, Gao J, Zhuge F, Liang L and Cao H 2018 *ACS Photonics* **5** 2094
- [38] Tiwari D, Alibhai D and Fermin D J 2018 *ACS Energy Lett.* **3** 1882

- [39] Liu X, Tan X, Liu Z, Ye H, Sun B, Shi T, Tang Z and Liao G 2019 *Nano Energy* **56** 184
- [40] Wang P, Zhang X, Zhou Y, Jiang Q, Ye Q, Chu Z, Li X, Yang X, Yin Z and You J 2018 *Nat. Commun.* **9** 2225
- [41] Chen W, Chen H, Xu G, Xue R, Wang S, Li Y and Li Y 2019 *Joule* **3** 191
- [42] Lin Z, Chen D, Hao Y, Chang J, Zhang C, Zhang J, Zhang Q, Zhu W and Zhang Z 2018 *Adv. Energy Mater.* **8** 1802080
- [43] Xiang W et al 2018 *Joule* **3** 205
- [44] Gupta S, Bendikov T, Hodes G and Cahen D 2016 *ACS Energy Lett.* **1** 1028
- [45] Bin Song T, Yokoyama T, Aramaki S and Kanatzidis M G 2017 *ACS Energy Lett.* **2** 897
- [46] Chen T et al 2019 *Nat. Commun.* **10** 16
- [47] Todorov T K, Singh S, Bishop D M, Gunawan O, Lee Y S, Gershon T S, Brew K W, Antunez P D and Haight R 2017 *Nat. Commun.* **8** 682
- [48] Xue D-J, Liu S-C, Dai C-M, Chen S, He C, Zhao L, Hu J-S and Wan L-J 2017 *J. Am. Chem. Soc.* **139** 958
- [49] Choi Y C, Lee D U, Noh J H, Kim E K and Seok S I L 2014 *Adv. Funct. Mater.* **24** 3587
- [50] Choi Y C, Lee Y H, Im S H, Noh J H, Mandal T N, Yang W S and Seok S I L 2014 *Adv. Energy Mater.* **4** 1301680
- [51] Whittaker-Brooks L, Gao J, Hailey A K, Thomas C R, Yao N and Loo Y-L 2015 *J. Mater. Chem. C* **3** 2686
- [52] Kauk-Kuusik M et al 2018 *Thin Solid Films* **666** 15
- [53] Spanier J E et al 2016 *Nat. Photon.* **10** 611
- [54] Guarnieri M 2015 *IEEE Ind. Electron. Mag.* **9** 58
- [55] Giraldo S, Jehl Z, Placidi M, Izquierdo-Roca V, Pérez-Rodríguez A and Saucedo E 2019 *Adv. Mater.* **31** 1806692
- [56] Zeng K, Xue D J and Tang J 2016 *Semicond. Sci. Technol.* **31** 1
- [57] Tang J 2019 private communication
- [58] Zakutayev A 2017 *Curr. Opin. Green Sustain. Chem.* **4** 8
- [59] Bosco J P 2014 *Rational Design of Zinc Phosphide Heterojunction Photovoltaics* (Pasadena, CA: California Institute of Technology)
- [60] Javaid K, Yu J, Wu W, Wang J, Zhang H, Gao J, Zhuge F, Liang L and Cao H 2018 *Phys. Status Solidi—Rapid Res. Lett.* **12** 1700332
- [61] Farrell R M, Neufeld C J, Cruz S C, Lang J R, Iza M, Keller S, Nakamura S, DenBaars S P, Mishra U K and Speck J S 2011 *Appl. Phys. Lett.* **98** 201107
- [62] Kulbak M, Cahen D and Hodes G 2015 *J. Phys. Chem. Lett.* **6** 2452
- [63] Eperon G E, Paternò G M, Sutton R J, Zampetti A, Haghghirad A A, Cacialli F and Snaith H J 2015 *J. Mater. Chem. A* **3** 19688
- [64] Ma Q, Huang S, Wen X, Green M A and Ho-Baillie A W Y 2016 *Adv. Energy Mater.* **6** 1502202
- [65] Xu H, Duan J, Zhao Y, Jiao Z, He B and Tang Q 2018 *J. Power Sources* **399** 76
- [66] Lejaeghere K et al 2016 *Science* **351** aad3000
- [67] Jain A et al 2013 *APL Mater.* **1** 011002
- [68] Yu L and Zunger A 2012 *Phys. Rev. Lett.* **108** 068701
- [69] Savory C N, Ganose A M and Scanlon D O 2017 *Chem. Mater.* **29** 5156
- [70] Hinuma Y et al 2016 *Nat. Commun.* **7** 11962
- [71] Blank B, Kirchartz T, Lany S and Rau U 2017 *Phys. Rev. Appl.* **8** 024032
- [72] Park J S, Kim S, Xie Z and Walsh A 2018 *Nat. Rev. Mater.* **3** 194
- [73] Alkauskas A, Yan Q and Van de Walle C G 2014 *Phys. Rev. B* **90** 075202
- [74] Kim S, Park J-S, Hood S N and Walsh A 2019 *J. Mater. Chem. A* **7** 2686